Food Hydrocolloids 139 (2023) 108481

Contents lists available at ScienceDirect

Food Hydrocolloids

journal homepage: www.elsevier.com/locate/foodhyd

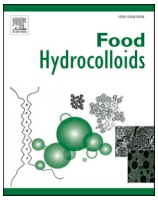

# Effects of viscoelasticity on moisture sorption of maltodextrins

R.G.M. van der Sman

*Wageningen-Food & Biobased Research, Wageningen University & Research, the Netherlands*

ARTICLE INFO

*Keywords:*
Hysteresis
Moisture sorption
Viscoelastic relaxation
Rheology
Numerical model

ABSTRACT

By means of a physically-based drying model we argue that hysteresis in moisture sorption of food materials can be explained by viscoelastic relaxation effects. The model is applied to maltodextrins, for which we have recently determined their rheology for conditions approaching the glassy state, as well as their moisture diffusion coefficients (which is shown to follow our earlier model for moisture diffusion). For these maltodextrins moisture sorption has been performed using the Dynamic Vapour Sorption (DVS) method. After an update of the earlier (sub)model for moisture diffusion with insights from aerosol drying, the model is shown to give reasonable predictions of the DVS experiments, which clearly exhibit the hysteresis in moisture sorption. The model was fitted to DVS data of four maltodextrins, differing in their DE-values. The independently determined fitting parameters showed a high degree consistency amongst the four maltodextrins, and they were close to some parameter values determined experimentally with rheology measurements. Via a parameter study we have performed a rough sensitivity study, showing significant effects of all model parameter. All the results of this study together makes us quite confident that viscoelastic relaxation effects is indeed the cause of hysteresis in moisture sorption, as has been argued earlier for solvent sorption of synthetic polymers.

## 1. Introduction

In this paper we investigate the hypothesis that hysteresis in moisture sorption of food materials is due to viscoelastic relaxation effects. Moisture sorption data is obtained from Dynamic Vapour Sorption (DVS) measurements on maltodextrins. Several studies have already addressed the modelling of DVS data of food material, but the majority of these studies model the moisture sorption with Fickian diffusion, often combined with the GAB moisture sorption theory (Besbes et al., 2013; Guillard et al., 2003; Kelly et al., 2016; Roca et al., 2008; Yu et al., 2008). Several authors stated that Fickian diffusion models break down near the glass transition (Enrione et al., 2007; Meinders & van Vliet, 2009; Zhao et al., 2019).

We argue that the Fickian diffusion approach is incomplete, as it does not account for mechanical stresses, and their relaxation, and (therefore) it can not explain the overshoots often observed in DVS experiments (Meinders & Oliver, 2015). For non-food materials non-Fickian diffusion models have been developed, but these are often phenomenological (Arhant et al., 2016; Popescu et al., 2014; Zhao et al., 2019). However, we strive for a mechanistic explanation for the moisture sorption, with 1) the moisture transport driven by a gradient in chemical potential, 2) inclusion of mechanical stresses in the chemical potential cf. Flory-Rehner theory, 3) the (self)diffusion described by a predictive theory, and 4) the relaxation of viscoelastic stresses following a model based on actual rheological data. This work builds on our earlier works, where we have addressed various elements of the above said approach (van Der Sman, 2013; Van der Sman et al., 2022, 2022van der Sman et al., 2023; Van der Sman & Meinders, 2011, 2013).

The hypothesis, that hysteresis is governed by viscoelastic effects, has been formerly formulated for cell wall materials (Hill & Xie, 2011), wood (Popescu et al., 2014), parchement (Popescu et al., 2016) and wool (Ormondroyd et al., 2017; Salmén & Larsson, 2018), and it is probably also applicable to food materials (Champion et al., 2011, 2011van der Sman et al., 2013; Zhang et al., 2015).

We will investigate the hypothesis for the case of maltodextrins, for which we have determined its viscoelastic behaviour for a wide range of temperatures, moisture contents, frequencies (shear rates) and molecular length (Siemons et al., 2022a; Van der Sman et al., 2022). Maltodextrins are an obvious choice, because such rheological data over such a wide range of parameters is much lacking over other food materials Kokini (1994); Ubbink and Dupas-Langlet (2020). But, this wide range is required for the mechanistic modelling of moisture sorption of the complete water activity range ($0 < a_w < 1$).

In their glassy state the maltodextrins attain very large value of the elastic modulus in the order of 1 GPa, accompanied by large relaxation times. Hence, during drying large elastic stresses can be developed,

*E-mail address:* ruud.vandersman@wur.nl.

https://doi.org/10.1016/j.foodhyd.2023.108481
Received 28 October 2022; Received in revised form 23 December 2022; Accepted 11 January 2023
Available online 19 January 2023

which will not be dissipated over practical time scales (Okuzono & Doi, 2008). Hence, during drying elastic stresses can be locked in the biopolymer matrix, if it has reached the glassy state.

Similar to the case of gels, as formulated by the Flory-Rehner theory, the elastic stresses have to be incorporated in the thermodynamics governing the interaction of biopolymers with water (Van der Sman, 2015a). Next to the mixing contribution, as described by Flory-Huggins theory, the chemical potential of water attains a second contribution linear in the elastic stress. This extra term must be accounted for in the physical theories of moisture sorption of biopolymers and in physical models of food materials drying. However, this contribution is lacking in most of the theories on moisture sorption, with the exception of the theory of Leibler and Sekimoto (Leibler & Sekimoto, 1993). The so-called Free-Volume theory of Vrentas and Vrentas also accounts for an extra contribution due to structural ($\alpha$) relaxation in the chemical potential of water, but it is not directly formulated in terms of the mechanical properties (Vrentas & Vrentas, 1996).

At temperatures above the glass transition maltodextrins behave as viscoelastic materials, where elastic stresses are dissipated over a certain distribution of relaxation times. For maltodextrins we have shown there are two independent structural relaxation process: 1) a single relaxation time Maxwell mode, and 2) structural $\alpha$-relaxations with a broad spectrum of relaxation times (Siemons et al., 2022a; Van der Sman et al., 2022). The Maxwell mode is only present at sufficient molecular length of the maltodextrin, allowing it to form crystalline junctions, acting as physical crosslinks. All maltodextrins exhibit $\alpha$-relaxations, related to the stiffening of the material as it nears the glass transition. We expect the $\alpha$-relaxations can be attributed to hydrogen bonding, which strongly correlates with $T_g$ and viscosity (Van der Sman, 2013; Van der Sman et al., 2022, 2022van der Sman & Mauer, 2019). We expect that viscoelasticity will exhibits its effect during dynamic vapour sorption measurements (Meinders & Oliver, 2015; Oliver & Meinders, 2011). Consequently, near the glassy state where the relaxation times get longer, it becomes difficult to achieve equilibrium conditions and thus accurate $a_w$ measurements.

In this paper we construct a physical model describing the dynamic vapour sorption (DVS) of maltodextrins, incorporating the viscoelastic effects. The submodel for diffusion will be partly updated with the fact that the self-diffusion of water in glassy matrices kind of levels off, as found in aerosols made up with sugars (Ingram et al., 2017; Lienhard et al., 2014; Zobrist et al., 2011). Earlier, we have described the water activity with the Flory-Huggins-Free-Volume theory (FHFV), which extends the classical Flory-Huggins theory for polymers with an extra Free-Volume terms if the material is in the glassy state, cf. (Vrentas & Vrentas, 1991). In the current model we will replace the free volume term with the elastic stress contribution, cf. Flory-Rehner theory. The rheology of maltodextrins has been characterized via dynamic viscoelasticity measurements (frequency sweeps), which is described via the complex modulus as a function of frequency. This has to be converted into a time-dependent model of the elastic stress. For the Maxwell mode, we can use the Maxwell model straightforward, but actually for the $\alpha$-relaxations we can use a fractional derivative model, cf. (Faber et al., 2017; Jakobsen et al., 2011; Ng & McKinley, 2008), but we take a numerical approximation via a Prony series.

However, the (generalized) Maxwell viscoelastic models are developed for small strain deformations, while during DVS measurements the deformations can be beyond the linear regime. We will develop viscoelastic models for large deformations, using a set of internal variables, both for the Maxwell mode and the structural relaxations. Large deformations are defined in relation to a reference length, where the elastic stresses are zero. The internal variables are related to these reference lengths. These reference lengths will relax towards to the current deformation state with a certain relaxation time.

We note that similar models, coupling solvent transport, stress and viscoelastic relaxation, have been developed to describe diffusion in glassy synthetic polymers, which exhibit so-called case-II diffusion (Doumenc et al., 2006; Durning, 1985; Wu & Peppas, 1993), which have already shown to be able to describe hysteresis in solvent adsorption (Doumenc et al., 2006; Liu et al., 1999). This study is the first application of such models to food materials, for which realistic rheological data over the complete water activity range is available.

## 2. Theory for moisture sorption in viscoelastic materials

### 2.1. Equilibrium properties

As an alternative of the FHFV theory, we develop a new theory where the extra contribution to moisture sorption in the glassy state is due to an elastic contribution. In absence of elastic stresses we assume that the chemical potential of food materials can be described by Flory-Huggins theory (Van der Sman, 2012, 2019; Van der Sman and Meinders, 2011, 2013). The Flory-Rehner theory shows how to link elastic stresses to moisture sorption. The moisture sorption is governed by the chemical potential, which can be decomposed in two independent parts:

$$\mu_w = RT\log(a_w) = \mu_{w,mix} + \mu_{w,elas} \tag{1}$$

The first contribution is due to mixing of ingredients with water, as follows from the Flory-Huggins theory. The mixing contribution can also be reformulated as an osmotic pressure: $\mu_{w,mix} = -\nu_w \Pi_{mix}$, with $\nu_w$ the molar volume of water.

The elastic contribution is due to elastic stresses in the material. For simplicity we assume that the deformation is isotropic, and the stress can be represented by a scalar: $\sigma = \Pi_{elas}$. The elastic contribution to the chemical potential can thus be rewritten as:

$$\mu_{w,elas} = \nu_w \Pi_{elas} \tag{2}$$

Flory-Rehner theory assumes isotropic and homogeneous deformation. Consequently, $\Pi_{elas}$ can be expressed in the relative volume change $1/\widetilde{\varphi} = \varphi_{ref}/\varphi_s = \lambda^3$ (Van der Sman, 2015b, 2015a). $\lambda$ is the so-called stretch parameter, which is the total deformation compared to the reference length. The relative volume change can also be expressed in terms of $\widetilde{\varphi} = \varphi_s/\varphi_{ref}$ with $\varphi_s$ the polymer volume fraction, and $\varphi_{ref}$ a reference value. For viscoelastic media it should hold that $\sigma = 0$ if $\lambda = 1$, i.e. if $\varphi_s = \varphi_{ref}$. As an alternative to the strain energy from the Flory-Rehner theory we use the model, originally applied to gelatin, by Si Chen (Chen et al., 2020), from which follows:

$$\sigma = G(\widetilde{\varphi}^{\frac{1}{3}} - \widetilde{\varphi}) \tag{3}$$

$G$ is the shear modulus. In contrast to the Flory-Rehner theory this model is consistent with the above requirement for viscoelastic media, that $\sigma(\widetilde{\varphi} = 1) = 0$.

### 2.2. Non-equilibrium properties

#### 2.2.1. Moisture transport

If the food material is not in equilibrium with the gas phase, i.e. $a_w \neq R.H.$, then there will be moisture transport. Inside the solid food material moisture transport is driven by gradients in the chemical potential. We will express the mass balance in terms of the volume fraction of water $\varphi_w$:

$$\partial_t \varphi_w = -\nabla \cdot \varphi_w u_w \tag{4}$$

$\varphi_w u_w$ is the volumetric moisture flux, linear in the velocity of moisture $u_w$ and $\varphi_w$. The moisture flux is due to diffusion, and the displacement by the biopolymer matrix due to swelling at velocity $u_s$. The diffusive flux is expressed in the drift velocity $u_w - u_s$:

$$j_w = \varphi_w(u_w - u_s) = -M\nabla\mu_w \tag{5}$$

$M$ is the mobility.

The mass balance can be rewritten as:

$$\partial_t \varphi_w + \nabla\cdot\varphi_w u_s = \nabla M\cdot\nabla\mu_w \tag{6}$$

The above mass balance is expressed in the stationary Eulerian framework. Recall that the left hand side is the material derivative in the Lagrangian framework, moving along with the deforming biopolymer matrix. In the Lagrangian framework only the diffusive moisture flux is exchanged between control volume elements, but the control volume elements can change in volume and position (Räderer et al., 2002). Below, we will implicitly assume all equations will be solved in the Lagrangian framework, and time derivative implies the material derivative.

There are no predictive theories for the mobility $M$ of water in food materials. Hence, it advantageous to rewrite the diffusive flux as Fick's law:

$$j_w = -M\nabla\mu_w = -D_m\nabla\varphi_w \tag{7}$$

$D_m$ is the mutual diffusion coefficient, for which we have developed a predictive theory (Van der Sman & Meinders, 2013). The theory is tested for multiple carbohydrates like disaccharides and maltodextrins (Perdana et al., 2014; Siemons et al., 2019; Thirunathan et al., 2018; Van der Sman & Meinders, 2013). The relation between the mutual diffusion coefficient and mobility is (Hong et al., 2008):

$$M = \frac{D_m \nu_w}{RT} \tag{8}$$

In the glassy state Vrentas expect that the diffusion coefficient is relatively composition independent (Vrentas et al., 1975), which is consistent with the observation by Zobrist for sucrose aerosols (Zobrist et al., 2011). Other recent measurement of water diffusion in sucrose aerosols suggest that the original (free volume) theory predict much too low diffusion coefficients in the glassy state. Below, we give an adaption of the theory for the glassy state, which is consistent with these recent results.

### 2.2.2. Viscoelastic relaxation

The classical model for small deformations of viscoelastic media is by Maxwell, which is as follows:

$$\sigma + \tau_0\frac{d\sigma}{dt} = G\tau_0\frac{d\varepsilon}{dt} \tag{9}$$

The Fourier transform of this equation is

$$\sigma^* + i\omega\tau_0\sigma^* = G(i\omega\tau_0)\varepsilon^* \tag{10}$$

which can be rewritten as:

$$\sigma^* = G\frac{i\omega\tau_0}{1+i\omega\tau_0}\varepsilon^* \tag{11}$$

Another convenient way of writing the Maxwell model is as follows. The strain is decomposed in two parts: an elastic and inelastic one: $\varepsilon = \varepsilon^{el} + \varepsilon^{in}$. The stress is equal to $\sigma = G\varepsilon^{el}$, and the non equilibrium part relaxes as:

$$\frac{d\varepsilon^{in}}{dt} = \frac{\varepsilon - \varepsilon^{in}}{\tau_0} \tag{12}$$

The inelastic part of the deformation one can interpret as the internal variable as used in large deformation viscoelastic models (Holzapfel, 1996). There, the deformation is decomposed in an elastic and inelastic (viscous) part. The elastic energy, only depends on the elastic part. The inelastic energy dissipates, and it is described by a relaxation of the viscous deformation (Bosnjak et al., 2020; Chen & Ravi-Chandar, 2022).

We construct a large deformation version of the Maxwell model via interpreting $\varphi_{ref}$ as the internal variable, in the spirit of the visco-hyperelastic model for transient networks (Reese, 2003). We assume it relaxes as follows:

$$\frac{d\varphi_{ref}}{dt} = \frac{(\varphi - \varphi_{ref})}{\tau_0} \tag{13}$$

The elastic stress is computed as: $\sigma = G(\widetilde{\varphi}^{\frac{1}{3}} - \widetilde{\varphi})$.

In the Appendix we show with trial simulations and mathematical analysis show that in the limit of small deformations the above model is equivalent with the Maxwell model.

The physical picture of the relaxing reference length is akin to the transient network hypothesis (Dal et al., 2020), proposed earlier by Tobolsky and Green, and extended by (Linder et al., 2011) where physical crosslinks (i.e. hydrogen bonds) are constantly broken and formed. $\varphi_{ref}^{-\frac{1}{3}}$ can be related to the distance between these physical crosslinks, which can slip along the polymer backbone due to the mechanical deformations. In the view of the transient network model (Reese, 2003) the internal variable, $\varphi_{ref}$, corresponds to an intermediate reference frame, where the elastic stress is always zero. A hyperelastic theory, the dry state is often taken as the reference state. For polymers in the dry state holds of course: $\varphi_s = \varphi_{dry} = 1$. The definition of the intermediate reference state implies a multiplicative decomposition, akin to viscohyperelastic models:

$$\frac{\varphi_s}{\varphi_{dry}} = \frac{\varphi_s}{\varphi_{ref}}\frac{\varphi_{ref}}{\varphi_{dry}} \tag{14}$$

The first contribution is related to the elastic deformation: $\widetilde{\varphi} = \varphi_s/\varphi_{ref}$ and the latter part is related to the inelastic deformation $\varphi_{ref}/\varphi_{dry}$.

Viscoelastic relaxation of biopolymers is quite complex, and the Maxwell model does not suffice. Maltodextrin viscoelastic properties can be described by the Marin-Graessley model. A master curve of the elastic and loss modulus is shown in Fig. 1.

The spectrum is conveniently expressed in terms of the complex modulus $G^* = \sigma^*/\varepsilon^*$.

$$G^*(\omega) = G_N\frac{i\omega\tau_0}{1+i\omega\tau_0} + G_\infty\frac{(i\omega\tau_\beta)^\beta}{1+(i\omega\tau_\beta)^\beta} \tag{15}$$

Previously, we have formulated the model in terms of the compliance ($J^* = 1/G^*$), with parameters as shown in Fig. 1. We have define $\tau_0 = \tau_M(G_N/G_\infty)$ and $\tau_\beta = \tau_\alpha(G_\infty/G_N)^{1/\beta}$.

The first term is a Maxwell relaxation mode, as follows from the Fourier transform. The second term is a Cole-Cole model, which is the Fourier transform of a fractional derivative model. The above Marin-Graessley model can be related to the fractional Zener model (Xiao et al., 2016). As above, the strain $\varepsilon$ is divided in an elastic) and inelastic (viscous) part $\varepsilon = \varepsilon_{el} + \varepsilon_{in}$. The inelastic part evolves as (Xiao et al., 2016):

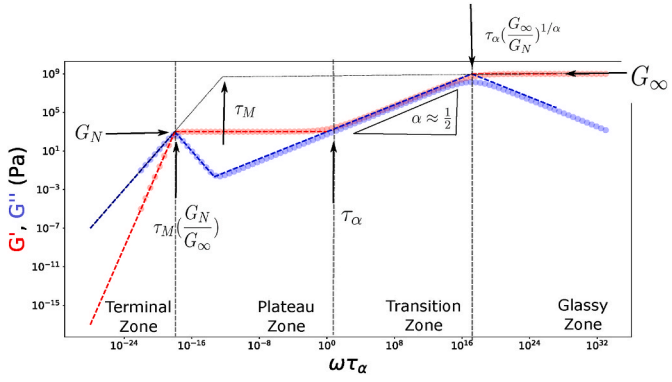


**Fig. 1.** Example of master curve produced by the Marin-Graessely model with explanation of the model parameters. In the terminal and plateau zone, the material behaves approximately as described by a Maxwell model. In the transition and glassy zone, the material behaves approximately as described by a Cole-Cole model.

$$\frac{d^\beta \varepsilon_{in}}{dt^\beta} = \frac{\varepsilon - \varepsilon_{in}}{\tau^\beta} \tag{16}$$

The elastic stress is:

$$\sigma = G_M \varepsilon + G_{neq}(\varepsilon - \varepsilon_{in}) \tag{17}$$

A large deformation version of the fractional Zener model is obtained via relaxation of a second internal variable $\varphi_{ref}$, as governed by the fractional derivative model:

$$\frac{d^\beta \varphi_{ref}}{dt^\beta} = \frac{\varphi - \varphi_{ref}}{\tau^\beta} \tag{18}$$

Computations with the fractional derivative models is highly complex and demanding. Hence, we will approximate the model with a Prony series, as described below.

#### 2.2.3. Approximation rheology by Prony series

The approximation of the relaxation spectrum of the Marin-Graessley model is via the following Prony series:

$$G^*(\omega) = G_N \frac{i\omega\tau_0}{1 + i\omega\tau_0} + \delta \sum_{i>0} G_i \frac{i\omega\tau_i}{1 + i\omega\tau_i} \tag{19}$$

The relaxation times $\tau_i$ are within the range $\tau_\alpha < \tau_i < \tau_\beta$, as commonly advised we take 2 relaxation modes per decade. The strength of the relaxation modes scale as:

$$G_i \sim (\omega\tau_\alpha)^\beta \tag{20}$$

with $G_N \leq G_i \leq G_\infty$. $\delta = O(1)$ is a parameter to maximize the goodness of fit between Marin-Graessly model and the Prony series approximation. For maltodextrin DE5, we have found that $G_\infty \approx 10^9$ Pa, and $G_N \approx 10^5$ Pa, $\alpha = 0.60$, $\tau_M/\tau_\alpha \approx 2000$. In Fig. 2 we compare the Marin-Graessley model for DE5 and the Prony series approximation. Good fit is obtained for $\delta \approx 0.38$. This value varies slightly for other values of $\alpha$.

We observe that in the terminal zone, the first part of the plateau zone, and the transition zone very good fits are obtained between both models. In regions where the fit is less good, $G'' \ll G'$. Hence, the response of the material is dominantly pure elastic, and the value of $G''$ is not very relevant. We proceed with this approximation.

In case of small deformations the Prony series approximation can be

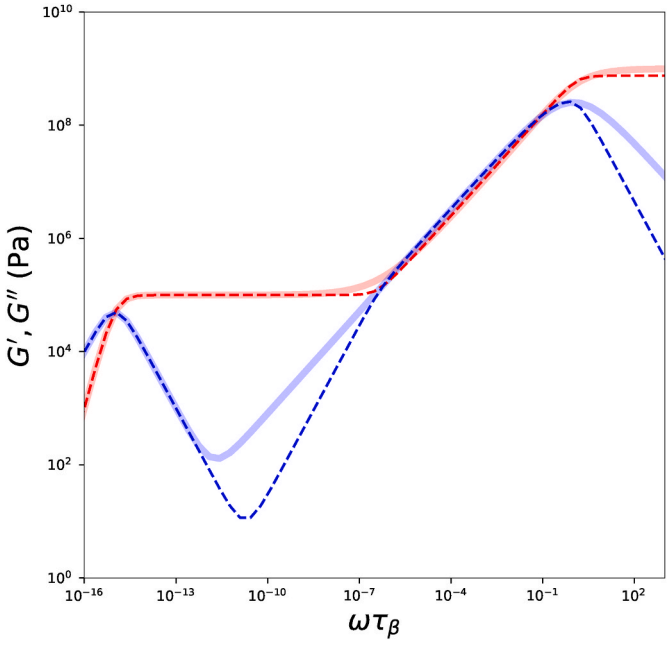


**Fig. 2.** Marin-Graessely model (thick solid lines) approximated by a Prony series (dashed lines). $G'$ is indicated in red, and $G''$ in blue.

implemented as a set of ode's:

$$\frac{d\varepsilon_i^{in}}{dt} = \frac{\varepsilon - \varepsilon_i^{in}}{\tau_i} \tag{21}$$

and $\sigma = \sum_i G_i \varepsilon_i^{el} = \sum_i G_i(\varepsilon - \varepsilon_i^{in})$. The Maxwell mode of the Marin-Graessly model also follows the same equation, with $i = 0$, $G_0 = G_N$ and $\tau_i \ll \tau_0$ (for $i > 0$). $\varepsilon_i^{neq}$ functions as internal variables, which relax with a breadth of relaxation times.

However, we will apply the Prony series approximation for the case of large deformations. We introduce the internal variables $\varphi_{g,i}$ which will relax with time constant $\tau_i$. The stress will be equal to:

$$\sigma = \sum_i G_i(\tilde{\varphi}_i^{\frac{1}{3}} - \tilde{\varphi}_i) \tag{22}$$

with $\tilde{\varphi}_i = \varphi_s/\varphi_{g,i}$. The internal variable relaxes as:

$$\frac{d\varphi_{g,i}}{dt} = \frac{\varphi_s - \varphi_{g,i}}{\tau_i} \tag{23}$$

## 3. Constitutive relations

### 3.1. Flory-Huggins theory

The mixing chemical potential of water in maltodextrins $\mu_{w,mix}$ is derived from the Flory-Huggins theory (Van der Sman & Meinders, 2011):

$$\frac{\mu_w}{RT} = \ln(\varphi_w) + \left(1 - \frac{1}{N_s}\right)(1 - \varphi_w) + \chi_{ws}(1 - \varphi_w)^2 \tag{24}$$

$\varphi_w$ is the volume fraction of water, $N_s$ is the ratio of molar volume of maltodextrin versus water, $\chi_{ws}$ is the interaction parameter.

For maltodextrins with degree of polymerization $DP > 2$ the interaction parameter is composition dependent, which is as follows (Van der Sman, 2019):

$$\chi_{ws} = \chi_0 + (\chi_1 - \chi_0)(1 - \varphi_w)^2 \tag{25}$$

$\chi_0 = 0.5$, which takes an universal value for all biopolymers. $\chi_1$ takes a specific values for each biopolymer. Values for maltodextrins are listed in a recent paper (Linnenkugel et al., 2022), but the composition dependency is disregarded there.

### 3.2. Glass transition

We assume that the glass transition of maltodextrin follow the Couchman-Karasz relation (Van der Sman & Meinders, 2011):

$$T_g = \frac{y_w \Delta c_{p,w} T_{g,w} + y_s \Delta c_{p,s} T_{g,s}}{y_w \Delta c_{p,w} + y_s \Delta c_{p,s}} \tag{26}$$

$y_s, y_w$ are the mass fraction of water and solute, $T_{g,w}$ is the glass transition of pure water, $T_{g,s}$ is the glass transition of the dry maltodextrin, $\Delta c_{p,i}$ is the change of the specific heat of compound $i$ across the glass transition. For water the following values hold: $T_{g,w} = 139$ K, and $\Delta c_{p,w} = 1.91$ kJ/kg.K. For (poly)saccharides we assume the universal value $\Delta C_{p,s} = 0.425$ kJ/kg.K.

The glass transition of the dry polymer $T_{g,s}$ depends on the molecular weight $M_{w,s}$ via the Fox-Flory relation (Van der Sman & Meinders, 2011):

$$T_{g,s} = T_{g,s}^\infty - \frac{a_{FF}}{M_{w,s}} \tag{27}$$

For the maltodextrins analyzed in this study we determined $T_{g,\infty} = 460$ K and $a_{FF} = 54$ K kg/mol (Siemons et al., 2020).

### 3.3. Diffusion coefficient

We have developed a predictive theory for moisture diffusion for various food compounds (Van der Sman & Meinders, 2013), which is based on the earlier work of He, Fowler and Toner (He et al., 2006). The adapted model has shown to be predictive for diffusivities $D_m > 10^{-14}$ m/s$^2$ (Perdana et al., 2014). Importantly, the theory predicts that the self-diffusion coefficient of water is independent of molecular weight of carbohydrates, but is only a function of the volume fraction of water and temperature, as is also shown via molecular dynamics (Limbach & Ubbink, 2008).

Recent studies suggest that diffusion coefficients level off upon reaching the glassy state for HPMC (Laksmana et al., 2008) and sucrose or citric acid aerosols (Lienhard et al., 2014; Price et al., 2015; Zobrist et al., 2011). This aspect is not predicted by the free-volume theory. We explain this discrepancy by the expansion of free volume in carbohydrates near the glassy state (Townrow et al., 2010; Van der Sman & Meinders, 2013), which is not accounted for in our theory.

We have assumed that in the glassy state the specific volume follows:

$$v_{spec} = \frac{y_w}{\rho_w(T)} + \frac{y_s}{\rho_s(T)} + \Delta v_{FV}\left(\frac{y_w - y_{w,g}}{y_{w,g}}\right)^2 \tag{28}$$

Here $y_{w,g}$ is the mass fraction of water at which the glass transition at temperature $T$. $\Delta v_{FV} = 0.02 \times 10^{-3}$ m$^3$/kg is a fitting parameter, which is fitted to specific volume data as collected in (Van der Sman & Meinders, 2013).

In our theory we have modified the self-diffusion coefficient of water $D_{s,w}$, which is related to the (mutual) diffusion coefficient via: $D_m = \varphi_s D_{s,w} + (1 - \varphi_s)D_{s,s}$, with $D_{s,s}$ the self-diffusion coefficient of the solute (maltodextrin). In the range of $a_w \leq 0.9$ the mutual diffusion coefficient is dominated by $D_{s,w}$. In the free volume theory the water self diffusion is following the relation:

$$\ln\frac{D_{s,w}}{D_{w,0}} = -\frac{\Delta E}{RT} - \gamma\frac{V_{cr}}{V_f} \tag{29}$$

for $T < T_g$ we modify the latter term:

$$\begin{aligned} \gamma\frac{V_{cr}}{V_f} &= \gamma\frac{V_{cr,ref}}{V_{f,ref}} + +0.87\Delta v_{FV}\left(\frac{y_w - y_{w,g}}{y_{w,g}}\right)^2 \\ \gamma\frac{V_{cr,ref}}{V_{f,ref}} &= \frac{y_w\widehat{V}_w^* + \zeta y_s\widehat{V}_s^*}{y_w(K_{ww}/\gamma)(K_{sw} - T_{g,w} + T) + y_s(K_{ws}/\gamma)(K_{ss} - T_{g,s} - T)} \end{aligned} \tag{30}$$

$\gamma V_{cr,ref}/V_{f,ref}$ is the value for $T > T_g$.

The modified theory is shown in Fig. 3, which is compared to several datasets from literature: $D_{s,s}$ for sucrose from Price (Price et al., 2016), $D_{s,w}$ for sucrose (Nadler et al., 2019; Price et al., 2016), $D_{s,w}$ for maltose (Zhu et al., 2011), and $D_m$ for sucrose from Zobrist (Zobrist et al., 2011), and glucose syrup (Normand et al., 2019). For $T > T_g$ we assume that $D_{s,w}$ holds universally for carbohydrates based on fructose/glucose monomers: sugars, maltodextrins, dextrans and starch (Perdana et al., 2014; Siemons et al., 2019; Ubbink et al., 2007; Van der Sman & Meinders, 2011). Our current model is well following the empirical model of Zobrist (Zobrist et al., 2011).

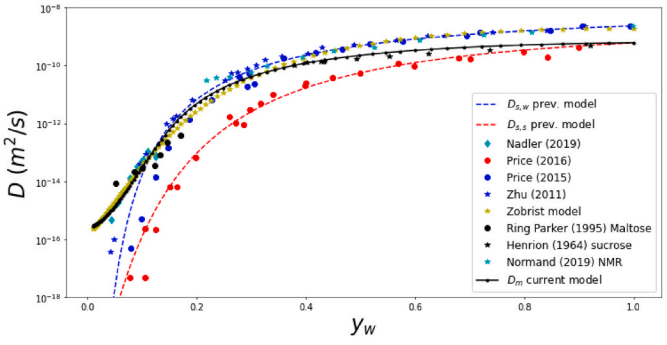


**Fig. 3.** Prediction of updated diffusion coefficient model as compared to experimental data for sucrose aerosols.

### 3.4. Maltodextrin rheology

From our recent paper (Siemons et al., 2022a) we reproduce the master curves, using the given $T_g$ as the reference temperature. The master curves are shown in Fig. 4.

The value of $\tau_\beta$ at the glass transition is often taken as $\tau_{\beta,g} = 100$ s (Dupas-Langlet et al., 2019; Maidannyk et al., 2017), assuming that DMA peak temperature coincides with the glass transition temperature. Other studies assume there might be difference. Hence, we will assume $\tau_{\beta,g}$ to be a fitting parameter.

The shift factors $a_T$ appears to be following the inverse of the zero shear viscosity $\eta_0$ (Van der Sman et al., 2022), as shown in Fig. 5. We follow that scaling. Due to absence of viscosity data for $T_g/T > 1$, we assume that $a_T$ is constant in that range, as suggested by the empirical shift factors in Fig. 5. This limiting value of $T_g/T$ is denoted as $(T_g/T)_{lim}$. Fig. 5 shows that there quite some uncertainty in the value of $TgT_{\lim}$, which we also assume to be a fit parameter.

## 4. Methods

### 4.1. Maltodextrin sorption

Measurements are performed using an automatic multi-sample moisture sorption analyzer SPSx-11$\mu$ (Project Messtechnik, Ulm, Germany), as described in (Erickson et al., 2014; Jin et al., 2014; Renzetti et al., 2012). In this equipment the relative humidity (RH) inside the climatic chamber is conditioned, and the instrument is equipped with a dew point analyzer to control RH, and a microbalance (WXS206SDU Mettler-Toledo, Greifensee, Switzerland) to measure sample weight.

Weight changes were measured at time intervals of 5 min. Samples were dried above P2O5 for 3 days before the DVS experiments. Initially, the $a_w$ of the powder was about $a_w \approx 0.1$. The sorption measurement procedure involved an initial drying at 30$^o$C for 500 min. First, the $a_w$ of the dry MDX powder is increased in two steps from 85% to 90%. Subsequently, the actual moisture desorption is measured, via decreasing the RH from 90% downto 0% in steps of 10%. Later, the moisture adsorption is measured via increasing the RH again to 90%, in steps of 10%. The minimal weight of the sample during the RH = 0% step is taken as the dry weight of the sample, with equilibration times at each stage in range 250 min$< t <$50 h. If equilibrium was reached for $t > 250$ min, we switched to the next stage. The equilibrium was determined when the weight change was less than 0.01% in three consecutive measurements.

Measurements were performed with maltodextrins with different DE (dextrose equivalents), namely DE = 5, DE = 12, DE = 21, and DE = 29. These are the same materials as we have used for the earlier rheological measurements (Siemons et al., 2022a).

### 4.2. Finite Volume method

The sample pan has a cylindrical shape. Hence, we have divided the system in N = 10 thin cylindrical control volumes. The (initial) height of the sample is determined from the initial mass, and the density of carbohydrates (Van der Sman & Meinders, 2013). We have assumed that after initial conditioning at RH = 85% all porosity is lost from the sample via collapse of the structure. We assumed no-flux boundary conditions on the bottom and side walls of the sample pan. This makes the diffusion effectively a one-dimensional problem. At the top of the sample we assume Dirichlet boundary conditions, with the surface always in equilibrium with the gas phase, whose RH is controlled by the DVS

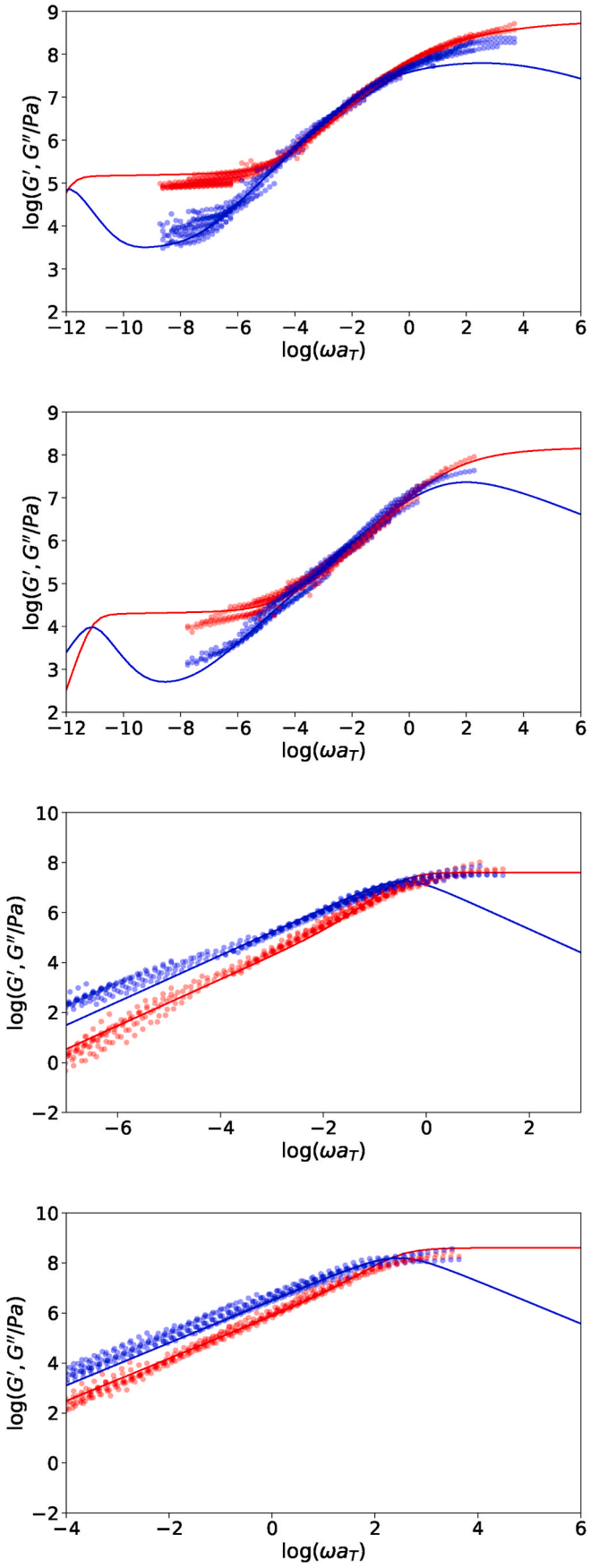


**Fig. 4.** Master curves of the rheology of maltodextrins fitted with the Marin-Graessely model. From top to bottom DE = 5, 12, 21 and 38.

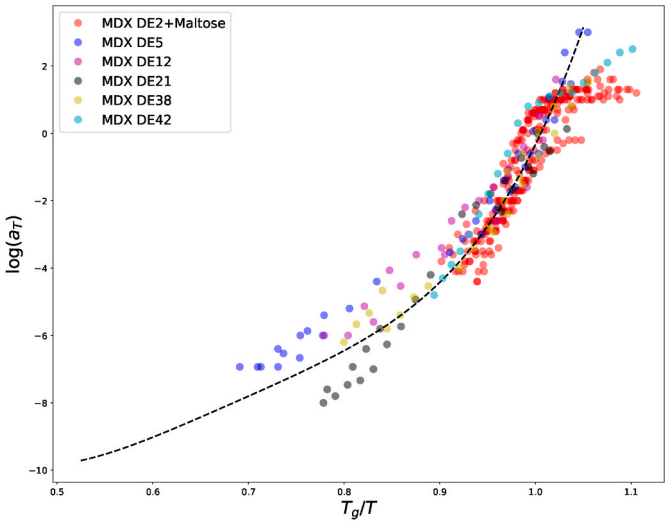


**Fig. 5.** Shift factors for maltodextrins follows that of the zero shear viscosity. Reproduced from (Van der Sman et al., 2022).

apparatus.

The moisture transport equation, Eqs. (6) and (7), is discretized using the Finite Volume method, using central differencing and explicit time integration. Shrinkage of the control volume due to moisture loss is taken into account, which implies only changes in the thickness. We do not consider any changes in the cross sectional area. After each time step the coordinates of each control volume is updated, cf. (Räderer et al., 2002), which is used for computing the gradients in the chemical potential. The mass fluxes are computed at the boundaries halfway between the centres of the control volumes. The corresponding diffusion coefficient is taken as the average of the diffusion coefficients in the two adjacent control volumes. The time step is adaptive, and is based on control volume with the largest diffusion coefficient $D_{\max}$, with thickness $\Delta x$: $\Delta t = Fo^* \Delta x^2 / D_{\max}$. The grid Fourier number is taken as $Fo^* = 0.06$.

For each control volume the stress is computed following Eq. (22). Each control volume has an independent set of internal variables $\varphi_{g,i}$, which evolve cf. Eq. (23). If the relaxation time $\tau_i < 80\Delta t$, we assume that the relaxation mode is at equilibrium: $\varphi_{g,i} = \varphi_s$.

## 5. Results

### 5.1. Prediction of DVS response and sorption isotherms

We performed simulations of the DVS response of for maltodextrin DE05, DE12, DE21, and DE29, following the above experimental protocol. The response of moisture content ($X_m$ on dry weight basis) as function of time is shown in Figs. 6–9. For each maltodextrins the DVS measurements are performed in duplicate, which are indicated via the green and blue curves in the figures. Model predictions are indicated in red. We note, that at low RH, it is difficult/impossible for the samples to reach equilibrium. If the samples are in the glassy state, the relaxation times become very long, and mechanical stresses can not be relaxed away in practical time scales. Consequently, a maximal "equilibration" time of 50 h was adopted in this range. For DE05 and DE12, we observe that even at intermediate RH it is difficult to obtain steady state values at the end of the "equilibration time". It is likely a consequence of the additional Maxwell mode the maltodextrins have (see Fig. 4). The effect of the Maxwell mode is significant if the material is in the rubbery state (i.e. the material behaves as a gel). The transition from the glassy to rubbery state happens at these intermediate RH.

The simulation results are obtained after optimization of model parameters. The parameter values corresponding with best fits are listed in

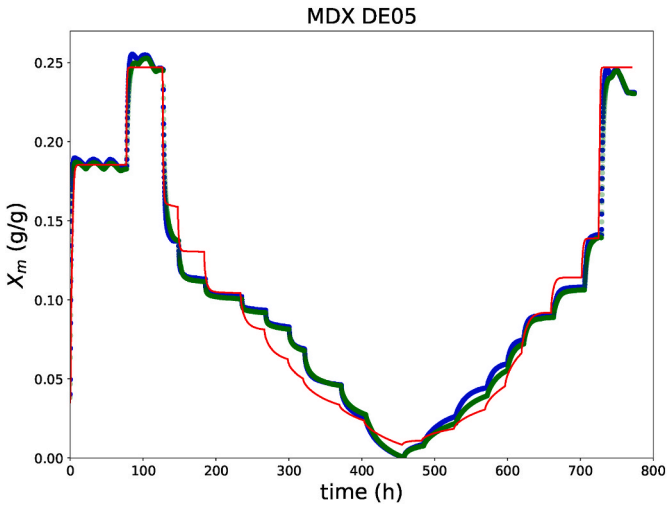


**Fig. 6.** Comparison between simulation and experiment of the dynamic moisture sorption of maltodextrin DE05. Green and blue curves indicate two experimental datasets (reproductions), and the red curve indicates the theoretical prediction.

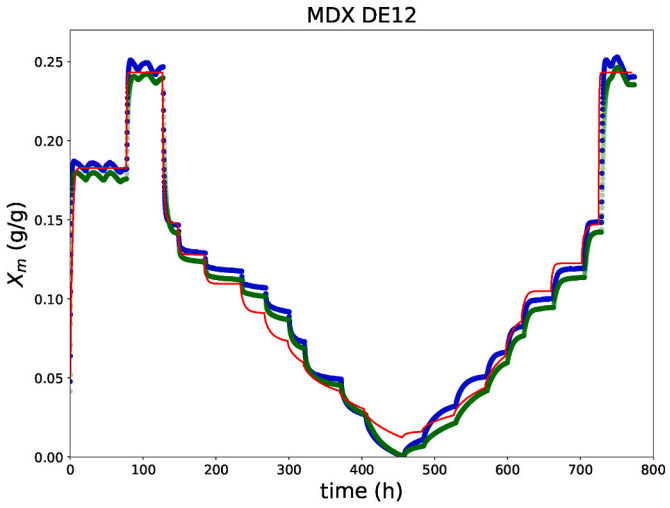


**Fig. 7.** Comparison between simulation and experiment of the dynamic moisture sorption of maltodextrin DE12. Green and blue curves indicate two experimental datasets (reproductions), and the red curve indicates the theoretical prediction.

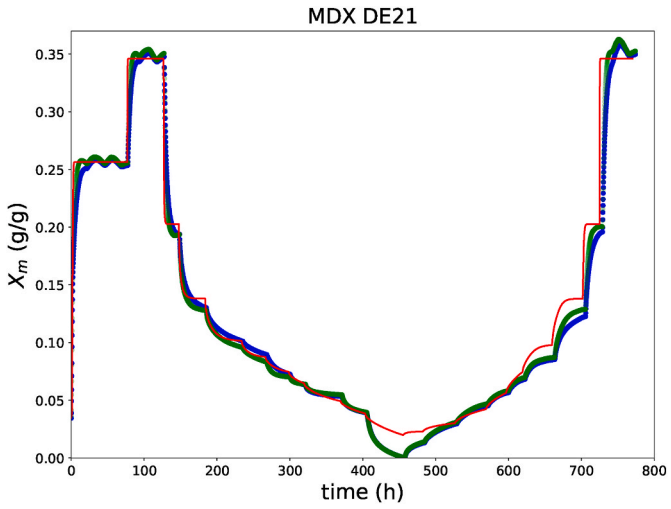


**Fig. 8.** Comparison between simulation and experiment of the dynamic moisture sorption of maltodextrin DE21. Green and blue curves indicate two experimental datasets (reproductions), and the red curve indicates the theoretical prediction.

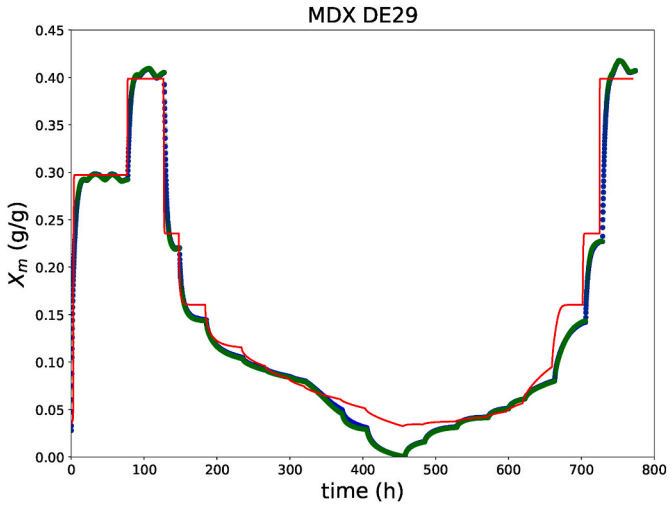


**Fig. 9.** Comparison between simulation and experiment of the dynamic moisture sorption of maltodextrin DE29. Green and blue curves indicate two experimental datasets (reproductions), and the red curve indicates the theoretical prediction.

Table 1. Due to long simulation times (more than 24 h) it was more practical to perform the optimization of the fitting by hand. Consequently, we have not be able to perform statistical analysis on the accuracy of model predictions. As an alternative, we will also perform a parameter study investigating the sensitivity of model predictions for parameter values.

From the DVS experiments and the simulations a sorption isotherm is constructed using the final moisture content values at the end of each step in RH. Comparison of experimental and predicted sorption isotherms are shown in Fig. 10. We observe that for DE21 and DE29 quite good predictions of the sorption hysteresis is obtained. Furthermore, the predictions of the DVS response for these maltodextrins is also close to the experimental values. The predictions of the hysteresis for DE05 and DE12 are slightly off, but the model captures the extend of the hysteresis reasonably well. We assume that this discrepancy between experiment and predictions are due to uncertainty in the initial stress state for DE05 and DE12. Their glass transitions are significantly higher than for DE21 and DE29, and consequently they enter the glassy state earlier during

**Table 1**
Fitting parameters.

| Compound | $T_g^\infty$ (K) | $\tau_{\beta,ref}$ (s) | $G_\infty$ (GPa) | $TgT_{\lim}$ | $\chi_{ws,1}$ |
|---|---|---|---|---|---|
| MDX DE05 | 445 | 1 | 0.2 | 1.06 | 1.21 |
| MDX DE12 | 445 | 4 | 0.4 | 1.06 | 1.22 |
| MDX DE21 | 445 | 4 | 0.7 | 1.06 | 0.97 |
| MDX DE29 | 445 | 4 | 0.8 | 1.06 | 0.83 |

the spray drying in their manufacturing. We assumed that initially all $\varphi_{g,i}$ are equal to the $\varphi_s$ in the glassy state (at room temperature). Of course the actual stress state might differ from this. Moreover, both DE05 and DE12 have an additional Maxwell mode, for which we do not know $\tau_M$ very accurately, as shown in Fig. 4.

The estimated parameter values, as listed in Table 1 are well within the expected ranges. $T_{g,\infty} = 445$ K, is close to the value of our previous experimental data, which showed $T_{g,\infty} = 460$ K (Siemons et al., 2022a). $\tau_{\beta,g} \approx 4$ s, while it is normally expected that $\tau_{\beta,g} \approx 100$s. This difference

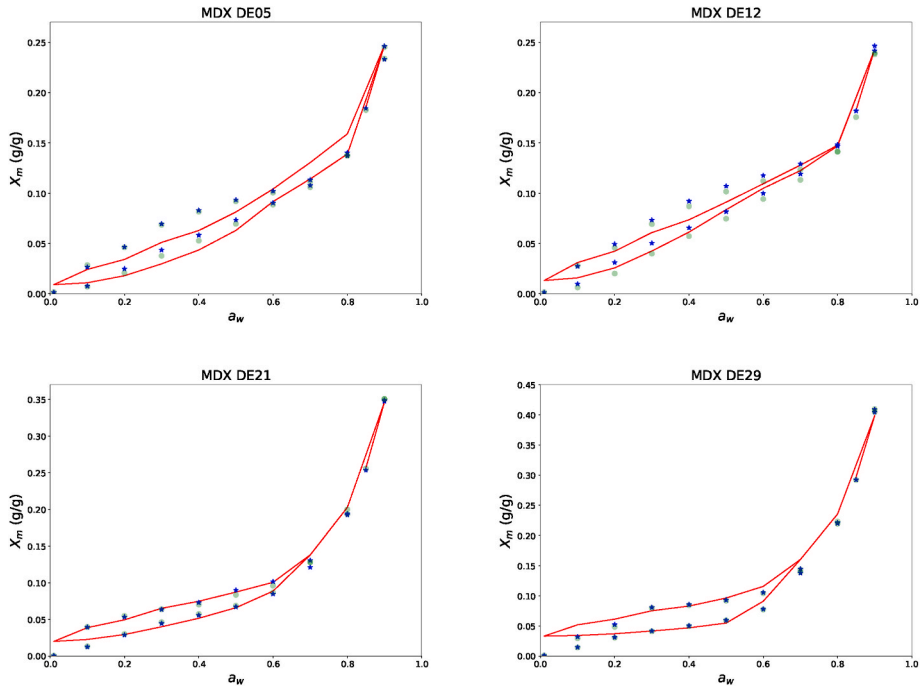


**Fig. 10.** Comparison between simulation and experiment regarding the hysteresis of MDX DE = 5–29.

can be due to the misconception that the peak in $G''$ in the glassy zone corresponds exactly with the glass transition temperature. $G_\infty$ is indeed of the order of 1 GPa, and $TgT_{\rm lim}$ is just above unity, as expected. The values of the Flory-Huggins interaction parameter are in similar range of those reported by (Linnenkugel et al., 2022). Differences in the $\chi$ values arise due to that (Linnenkugel et al., 2022) did not include composition dependency.

### 5.2. Parameter study

To show the sensitivity of the model for the fitting parameters we have performed a parameter study. As $T_{g,\infty}$ was quite consistent amongst the different maltodextrins, and with previous work we have chosen to keep this value fixed. The parameter study is performed for MDX DE21, for which the best fit was obtained.

Results are shown in Figs. 11–14. We observe that by varying $\tau_{\beta,g}$, $G_\infty$, and $TgT_{\rm lim}$ changes in moisture sorption only arise if the material

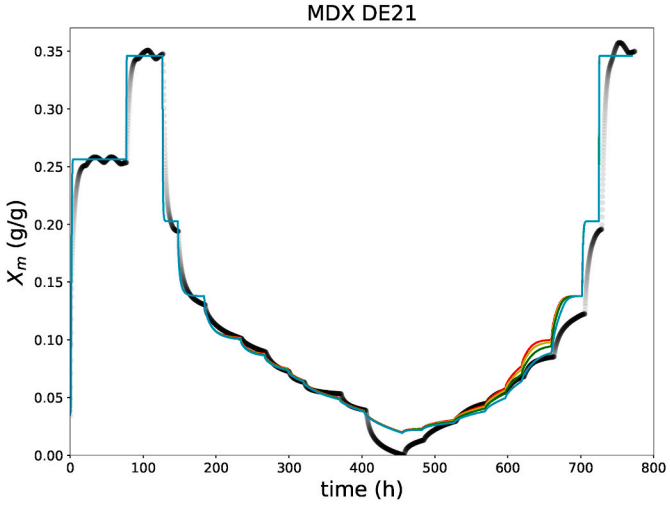


**Fig. 11.** Parameter study for MDX21 with $\tau_{\beta,g} = \{1, 2, 4, 8\}s$ (red to blue).

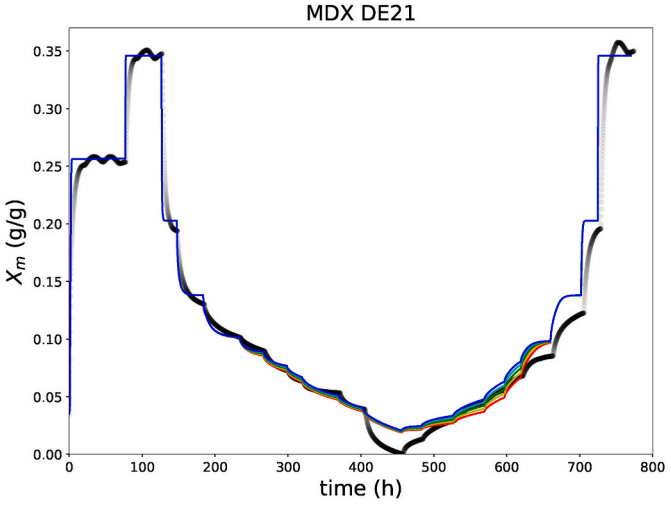


**Fig. 12.** Parameter study for MDX21 with $G_\infty = \{5, 6, 7, 8, 9\} \times 10^2$ MPa (red to blue).

gets into the glassy state. Moreover, the simulation results only significantly diverge during the adsorption phase. The responses are still very similar in the first desorption phase. Fig. 14 shows that variations in $\chi_1$ results in changes when the material is in the rubbery state, if $RH > 60\%$, but induces little changes in the glassy state.

If $TgT_{\rm lim} \geq 1.06$ the results do not change significantly, but results are strongly dependent on this parameter in the range $TgT_{\rm lim} < 1.06$. These changes are much larger than those induced by variation in $\tau_{\beta,g}$, $G_\infty$. Remarkably, for all maltodextrins we obtain good fitting results with $TgT_{\rm lim} = 1.06$. Because of this consistency, we assume this is the correct value for these maltodextrins.

Finally, to give an insight in the evolution of the viscoelastic relaxation times $\tau_{g,i}$ and internal variables $\varphi_{g,i}$, we have plotted them in Figs. 15 and 16. In Fig. 15 the bottom red line indicates $\tau_\alpha$. We observe that at high RH, the relaxation times immediately assume the new *equilibrium* values, but in the glassy state this evolution takes longer.

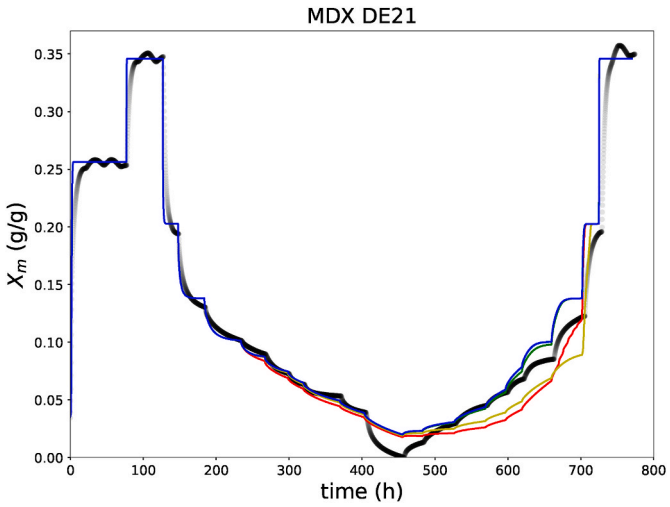


**Fig. 13.** Parameter study for MDX21 with $TgT_{\text{lim}} = \{1.04, 1.05, 1.06, 1.07, 1.08\}$ (red to blue).

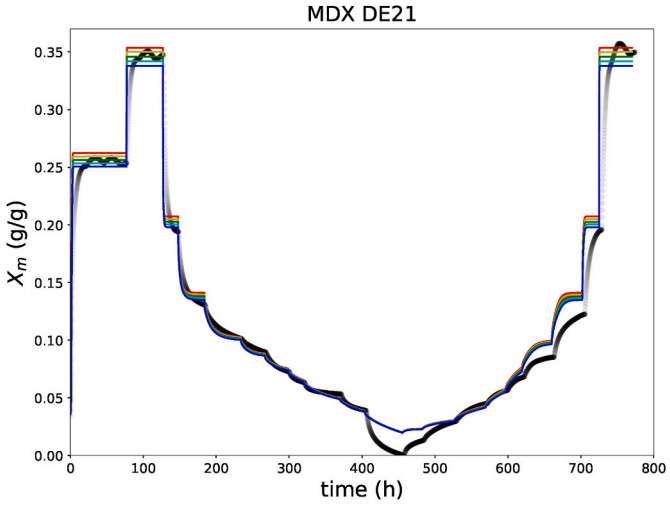


**Fig. 14.** Parameter study for MDX21 with $\chi_1 = \{0.95, 0.96, 0.97, 0.98, 0.99\}$ (red to blue).

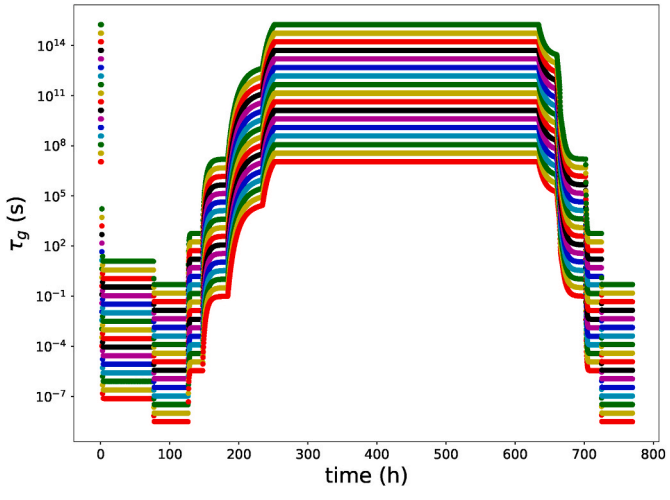


**Fig. 15.** Evolution of relaxation times $\tau_i$ during DVS experiment of MDX DE21, using best fit parameters. Bottom red line indicates $\alpha$-relaxation time $\tau_\alpha$. Other $\tau_i$ are multiples of $\tau_\alpha$.

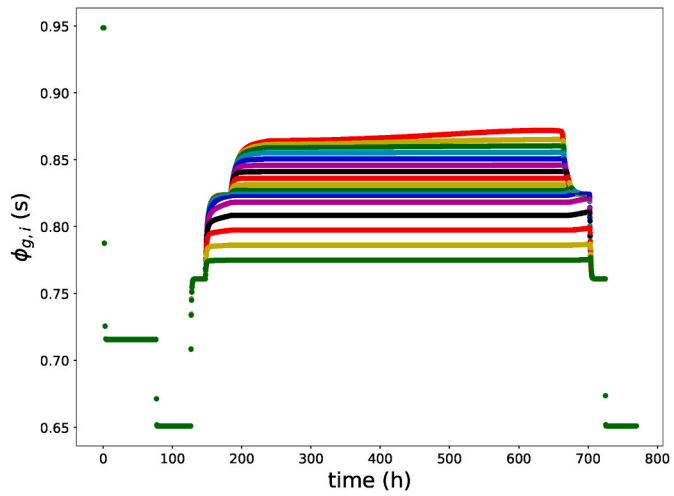


**Fig. 16.** Evolution of internal variables $\varphi_{g,i}$ during DVS experiment of MDX DE21, using best fit parameters. Top red line relaxes with $\tau_\alpha$ while the bottom green line relaxes with $\tau_\beta$.

Furthermore, if $TgT > TgT_{\text{lim}}$ we have truncated the relaxation times, which are all much longer than the experimental time scales ($\tau_{g,i} \gg 100$ $h$). Thus, effectively, the maltodextrin is behaving as an elastic solid. Similar behaviour is observed if we view Fig. 16. At high RH, if the material is in the rubbery state, all $\varphi_{g,i}$ easily follow $\varphi_s$. Approaching the glassy state the relaxation times become similar as the experimental time scales, and $\varphi_{g,i}$ start to deviate from $\varphi_s$. Soon, for modes with very long relaxation times, $\varphi_{g,i}$ becomes a constant. For the fast mode with $\tau_{g,i} = \tau_\alpha$ $\varphi_{g,i}$ is still changing if the material is deep into the glassy state. However, because of its small magnitude $G_i = G_N$ its contribution to stress and moisture sorption is negligible. The latter is more dominated by the slower modes, whose magnitudes are of order $G_\infty$. Similar reasoning holds for the significance of the Maxwell mode, for MDX DE05 and MDX12, whose magnitude $G_N$ is too small to have a significant impact on the moisture sorption isotherm, where $RH \leq 90\%$.

### 5.3. General discussion

Overall, based on the surprisingly good fits of the model with experimental data, and values of fitting parameters within expected ranges, we conclude that our model makes the case quite plausible that hysteresis in moisture sorption in food materials is due to viscoelastic relaxation of elastic stresses at very long time scales, prohibiting the material to acquire equilibrium conditions - which is in line with the statement of Nestle researchers in their recent paper (Dupas-Langlet et al., 2016). Practically, the material behaves as an elastic solid if $T_g/T > 1$, as in agreement with model of Leibler and Sekimoto (Leibler & Sekimoto, 1993). However, in the region just below the glas transition during adsorption viscoelastic effects on moisture sorption are not negligible. Hence, the Leibler-Sekimoto model will not capture the full effect of stresses on moisture sorption.

We gather that due to the complexity of the physics, readers do not directly grasp the implications of the viscoelastic phenomena of moisture sorption and its hysteresis. Hence, we summarize here the essence of the physics. For that, consider "equilibration" of the food material at a RH setpoint just above the glass transition. During desorption, the food material arrives at the setpoint from the rubbery state, where there is little stress build up, and which relaxes quickly away. We expect that during desorption the moisture content is near to the equilibrium value. During adsorption, the food materials arrives at the setpoint from the glassy state, where the material is nearly elastic. Consequently, during moisture (de)sorption in the glassy state some significant stresses have been build up. Due to the still long viscoelastic relaxation times in the

range between the glassy state and the RH setpoint, the stresses will not have relaxed away. As the water activity depends on both moisture and elastic stresses, the presence of stresses will lead to a different moisture content during the adsorption. Differences in the viscoelastic relaxation between desorption and adsorption are clearly observed in Figs. 15 and 16. Consequently, if the food material enters the glassy state during a DVS experiment they will exhibit hysteresis in moisture sorption due to the different histories in stress build up and its relaxation.

The presented model provides a physically-based alternative to the FHFV theory, we have used previously to describe moisture sorption of glassy food materials. However, for the new theory to apply one has to know the rheology of the material. Given the universal character of the FHFV theory, we expect a high degree of universality in the rheology of food materials in the transition and glassy zones. Results on glycerol solutions (Jensen et al., 2018) show that their rheology is described by models quite similar to the Marin-Graessley model, as used for maltodextrins. But, this universality of rheology has to be soundly established via further experiments.

In the region of RH $\approx$ 0% model predictions show significant deviation from experimental data. There are two possible explanations for this deviation: a) there is uncertainty in moisture diffusion coefficient in the glassy state (which is very difficult to measure), and b) the invalidity of the assumption that the minimal reading of the DVS at RH = 0% is without any moisture. Both experimental and simulation results show that steady state is not achieved in this region, and consequently it is likely at there is still moisture remaining in the food material at minimum of the DVS curve. Therefore, we advise to determine dry matter content via a separate way, p. e. via oven drying at temperatures above the glass transition (but below the decomposition temperature).

Due to the finding that equilibrium is hardly achieved at low RH, it is understandable that it is difficult to obtain consistent sorption isotherms from different literature sources, and thus obtain a consistent estimates of its parameters like $\chi_{ws}$, when comparing different fits (as done by (Linnenkugel et al., 2022)).

The significant effect of mechanical stress and viscoelastic relaxation on moisture sorption and transport will also play a role in other phenomena of food materials, near or in the glassy state. We assume mechanical stress is the dominant factor in the morphology development of droplet during spray drying (Siemons et al., 2020; 2022b). A similar model as presented in this paper must be used for the physical description of this phenomena, but also for regular description of (single) droplet drying during spray drying. Mechanical stresses have significant impact on the driving force for drying (i.e. the chemical potential $\mu_w$), and should be included in the drying models, as has been done recently for the case of drying aerosol droplets (Preston, 2022). Also, other models describing drying of non-edible soft matter include the mechanical stress in drying models (Bertrand et al., 2016; Chen et al., 2020; Christodoulou et al., 1998; Curatolo et al., 2018; Okuzono & Doi, 2008; Ozawa et al., 2006; Wang & Cai, 2015).

## 6. Conclusions

In this paper we presented a novel model for describing dynamics during moisture sorption. We think the presented results makes the case very plausible that hysteresis during moisture sorption can be explained by mechanical stresses and their viscoelastic relaxation. Near and in the glassy state viscoelastic relaxation times become very long compared to experimental time scale, resulting in the locking of mechanical stresses into the food material. This prohibits the glassy material to acquire equilibrium conditions, and the state of the material is highly dependent on the history of the material. These deviations accumulate during the time the material is in the glassy state. Especially, in the adsorption branch of the DVS these differences become apparent.

In the glassy state the material can be approximated by an elastic solid, but around the glass transition viscoelastic relaxation will also have a significant effect on moisture sorption. Hence, the Leibler-Sekimoto model, treating polymers as elastic solids, will not cover all physics governing moisture sorption near/in the glassy state.

In case of known rheology of food materials in the transition and glassy zones, the current model is a physically-based alternative for the Flory-Huggins-Free-Volume theory, we have used previously to describe moisture (ad)sorption of glassy food materials. We have indicated that similar models can be used for other drying problems in drying of foods or other soft matter.

## Author statement

I am the sole author, who has done all the writing. Contributions of others are acknowledged.

## Declaration of competing interest

I declare there are no conflicts of interest.

## Data availability

Data will be made available on request.

## Acknowledgements

I thank my colleague Stefano Renzetti of WFBR for performing the DVS experiments. Furthermore, I thank Gareth McKinley, MIT for fruitful discussions on fractional derivative models.

## Appendix. .AConsistency of viscohyperelastic and viscoelastic Maxwell model

We test the equivalence of our visco-hyperelastic model with the classical Maxwell model, in the limit of small deformations via trial simulations of a compression-stress relaxation test. Recall our definition of the Maxwell model:

$$\begin{aligned} \sigma &= G(\varepsilon - \varepsilon^{in}) \\ \frac{d\varepsilon^{in}}{dt} &= \frac{\varepsilon - \varepsilon^{in}}{\tau_0} \end{aligned} \tag{A.1}$$

and our viscohyperelastic Maxwell model is:

$$\begin{aligned} \sigma &= G\left(\tilde{\varphi}^{\frac{1}{3}} - \tilde{\varphi}\right) \\ \frac{d\varphi_{ref}}{dt} &= \frac{\varphi - \varphi_{ref}}{\tau_0} \end{aligned} \tag{A.2}$$

Assuming uniform compression (for example via immersion in an osmotic solution) Hence, $\varphi \sim 1/\lambda^3$ $\varphi_{ref} \sim 1/\lambda_{in}^3$, and $\tilde{\varphi} \sim 1/\lambda_{el}^3$ $\lambda_i = 1 + \varepsilon_i$ are the

so-called stretch parameters. Substitution of the definitions of the stretch parameters into the viscohyperelastic model gives:

$$\begin{aligned} \sigma &= \widetilde{G}(1/\lambda_e - 1/\lambda_e^3) \\ \frac{d1/\lambda_{in}}{dt} &= \frac{1/\lambda^3 - 1/\lambda_{in}^3}{\widetilde{\tau}_0} \end{aligned} \tag{A.3}$$

In the limit of small deformations, and taking only the linear terms in the Taylor expansion:

$$\begin{aligned} \sigma &= 2\widetilde{G}\varepsilon_{el} \\ \frac{\varepsilon_{in}}{dt} &= \frac{3(\varepsilon - \varepsilon_{in})}{\widetilde{\tau}_0} \end{aligned} \tag{A.4}$$

The models are equivalent if $2\widetilde{G} = G$, and $\frac{1}{3}\widetilde{\tau}_0 = \tau_0$. We have simulated a compression with a small displacement $\varepsilon_0 = 1\%$. The duration of the compression phase is $t_c = 3\tau_0$. Subsequently, the stress is computed while keeping the deformation constant at $\varepsilon_0$. Simulation results are shown in figure A17.

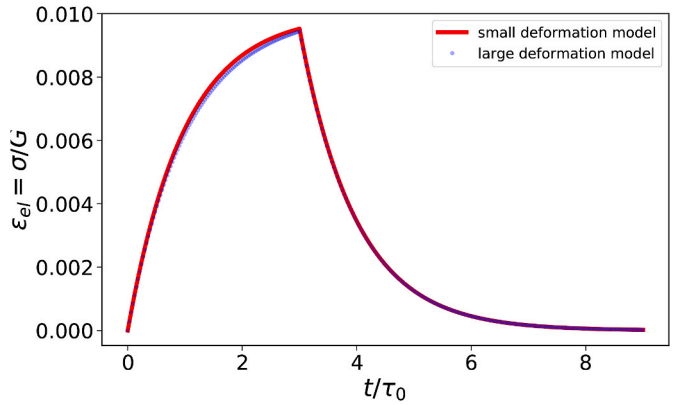


**Fig. A.17.** Equivalence of small and large deformation Maxwell model, with a single relaxation time $\tau_0$, using a simulation of a compression-relaxation experiment.

## References


Arhant, M., Le Gac, P. Y., Le Gall, M., Burtin, C., Briançon, C., & Davies, P. (2016). Modelling the non fickian water absorption in polyamide 6. *Polymer Degradation and Stability, 133*, 404–412.

Bertrand, T., Peixinho, J., Mukhopadhyay, S., & MacMinn, C. W. (2016). Dynamics of swelling and drying in a spherical gel. *Physical Review Applied, 6*, Article 064010.

Besbes, E., Jury, V., Monteau, J. Y., & Le Bail, A. (2013). Water vapor transport properties during staling of bread crumb and crust as affected by heating rate. *Food Research International, 50*, 10–19.

Bosnjak, N., Nadimpalli, S., Okumura, D., & Chester, S. A. (2020). Experiments and modeling of the viscoelastic behavior of polymeric gels. *Journal of the Mechanics and Physics of Solids, 137*, Article 103829.

Champion, D., Loupiac, C., Simatos, D., Lillford, P., & Cayot, P. (2011). Structural relaxation during drying and rehydration of food materials—the water effect and the origin of hysteresis. *Food Biophysics, 6*, 160–169.

Chen, S., Huang, R., & Ravi-Chandar, K. (2020). Linear and nonlinear poroelastic analysis of swelling and drying behavior of gelatin-based hydrogels. *International Journal of Solids and Structures, 195*, 43–56.

Chen, S., & Ravi-Chandar, K. (2022). Nonlinear poroviscoelastic behavior of gelatin-based hydrogel. *Journal of the Mechanics and Physics of Solids, 158*, Article 104650.

Christodoulou, K., Lightfoot, E., & Powell, R. (1998). Model of stress-induced defect formation in drying polymer films. *AIChE Journal, 44*, 1484–1498.

Curatolo, M., Nardinocchi, P., & Teresi, L. (2018). Driving water cavitation in a hydrogel cavity. *Soft Matter, 14*, 2310–2321.

Dal, H., Gültekin, O., & Açıkgöz, K. (2020). An extended eight-chain model for hyperelastic and finite viscoelastic response of rubberlike materials: Theory, experiments and numerical aspects. *Journal of the Mechanics and Physics of Solids, 145*, Article 104159.

van Der Sman, R. (2013). Predictions of glass transition temperature for hydrogen bonding biomaterials. *The Journal of Physical Chemistry B, 117*, 16303–16313.

Doumenc, F., Guerrier, B., & Allain, C. (2006). Aging and history effects in solvent-induced glass transition of polymer films. *EPL, 76*, 630.

Dupas-Langlet, M., Dupas, J., Samain, S., Giardiello, M. I., Meunier, V., & Forny, L. (2016). A new method to determine "equilibrated" water activity and establish sorption isotherm by erasing surface history of the samples. *Journal of Food Engineering, 184*, 53–62.

Dupas-Langlet, M., Meunier, V., Pouzot, M., & Ubbink, J. (2019). Influence of blend ratio and water content on the rheology and fragility of maltopolymer/maltose blends. *Carbohydrate Polymers, 213*, 147–158.

Durning, C. (1985). Differential sorption in viscoelastic fluids. *Journal of Polymer Science Polymer Physics Edition, 23*, 1831–1855.

Enrione, J. I., Hill, S. E., & Mitchell, J. R. (2007). Sorption and diffusional studies of extruded waxy maize starch-glycerol systems. *Starch Staerke, 59*, 1–9.

Erickson, D. P., Renzetti, S., Jurgens, A., Campanella, O. H., & Hamaker, B. R. (2014). Modulating state transition and mechanical properties of viscoelastic resins from maize zein through interactions with plasticizers and co-proteins. *Journal of Cereal Science, 60*, 576–583.

Faber, T., Jaishankar, A., & McKinley, G. H. (2017). Describing the firmness, springiness and rubberiness of food gels using fractional calculus. part i: Theoretical framework. *Food Hydrocolloids, 62*, 311–324.

Guillard, V., Broyart, B., Bonazzi, C., Guilbert, S., & Gontard, N. (2003). Preventing moisture transfer in a composite food using edible films: Experimental and mathematical study. *Journal of Food Science, 68*, 2267–2277.

He, X., Fowler, A., & Toner, M. (2006). Water activity and mobility in solutions of glycerol and small molecular weight sugars: Implication for cryo-and lyopreservation. *Journal of Applied Physics, 100*, Article 074702.

Hill, C. A., & Xie, Y. (2011). The dynamic water vapour sorption properties of natural fibres and viscoelastic behaviour of the cell wall: Is there a link between sorption kinetics and hysteresis? *Journal of Materials Science, 46*, 3738–3748.

Holzapfel, G. A. (1996). On large strain viscoelasticity: Continuum formulation and finite element applications to elastomeric structures. *International Journal for Numerical Methods in Engineering, 39*, 3903–3926.

Hong, W., Zhao, X., Zhou, J., & Suo, Z. (2008). A theory of coupled diffusion and large deformation in polymeric gels. *Journal of the Mechanics and Physics of Solids, 56*, 1779–1793.

Ingram, S., Cai, C., Song, Y. C., Glowacki, D. R., Topping, D. O., O'Meara, S., & Reid, J. P. (2017). Characterising the evaporation kinetics of water and semi-volatile organic compounds from viscous multicomponent organic aerosol particles. *Physical Chemistry Chemical Physics, 19*, 31634–31646.

Jakobsen, B., Niss, K., Maggi, C., Olsen, N. B., Christensen, T., & Dyre, J. C. (2011). Beta relaxation in the shear mechanics of viscous liquids: Phenomenology and network modeling of the alpha-beta merging region. *Journal of Non-crystalline Solids, 357*, 267–273.

Jensen, M. H., Gainaru, C., Alba-Simionesco, C., Hecksher, T., & Niss, K. (2018). Slow rheological mode in glycerol and glycerol–water mixtures. *Physical Chemistry Chemical Physics, 20*, 1716–1723.

Jin, X., van der Sman, R., van Maanen, J., van Deventer, H., van Straten, G., Boom, R., & van Boxtel, A. (2014). Moisture sorption isotherms of broccoli interpreted with the flory-huggins free volume theory. *Food Biophysics, 9*, 1–9.

Kelly, G. M., O'Mahony, J. A., Kelly, A. L., & O'Callaghan, D. J. (2016). Water sorption and diffusion properties of spray-dried dairy powders containing intact and hydrolysed whey protein. *LWT–Food Science and Technology, 68*, 119–126.

Kokini, J. (1994). Predicting the rheology of food biopolymers using constitutive models. *Carbohydrate Polymers, 25*, 319–329.

Laksmana, F. L., Kok, P. J. H., Frijlink, H. W., Vromans, H., & Van der Voort Maarschalk, K. (2008). Using the internal stress concept to assess the importance of moisture sorption-induced swelling on the moisture transport through the glassy hpmc films. *AAPS PharmSciTech, 9*, 891–898.
Leibler, L., & Sekimoto, K. (1993). On the sorption of gases and liquids in glassy polymers. *Macromolecules, 26*, 6937–6939.
Lienhard, D. M., Huisman, A. J., Bones, D. L., Te, Y. F., Luo, B. P., Krieger, U. K., & Reid, J. P. (2014). Retrieving the translational diffusion coefficient of water from experiments on single levitated aerosol droplets. *Physical Chemistry Chemical Physics, 16*, 16677–16683.
Limbach, H., & Ubbink, J. (2008). Structure and dynamics of maltooligomer–water solutions and glasses. *Soft Matter, 4*, 1887–1898.
Linder, C., Tkachuk, M., & Miehe, C. (2011). A micromechanically motivated diffusion-based transient network model and its incorporation into finite rubber viscoelasticity. *Journal of the Mechanics and Physics of Solids, 59*, 2134–2156.
Linnenkugel, S., Paterson, A. H., Huffman, L. M., & Bronlund, J. (2022). *Prediction of the effect of water on the glass transition temperature of low molecular weight and polysaccharide mixtures*. Food Hydrocolloids, Article 107573.
Liu, H., Li, J., & Hu, Y. (1999). A transport model for sorption and desorption of penetrants in glassy polymer membrane. *Fluid Phase Equilibria, 158*, 1035–1044.
Maidannyk, V., Nurhadi, B., & Roos, Y. (2017). Structural strength analysis of amorphous trehalose-maltodextrin systems. *Food Research International, 96*, 121–131.
Meinders, M., & Oliver, L. (2015). Viscoelastic sorption behavior of starch and gluten. In *Water stress in biological, chemical, pharmaceutical and food systems* (pp. 149–159). Springer.
Meinders, M. B., & van Vliet, T. (2009). Modeling water sorption dynamics of cellular solid food systems using free volume theory. *Food Hydrocolloids, 23*, 2234–2242.
Nadler, K. A., Kim, P., Huang, D. L., Xiong, W., & Continetti, R. E. (2019). Water diffusion measurements of single charged aerosols using h 2 o/d 2 o isotope exchange and Raman spectroscopy in an electrodynamic balance. *Physical Chemistry Chemical Physics, 21*, 15062–15071.
Ng, T. S., & McKinley, G. H. (2008). Power law gels at finite strains: The nonlinear rheology of gluten gels. *Journal of Rheology, 52*, 417–449.
Normand, V., Armanet, L., McIver, R. C., & Bouquerand, P. E. (2019). Water diffusion in the semi-liquid state during industrial candy preparation. *Food Biophysics, 14*, 193–204.
Okuzono, T., & Doi, M. (2008). Effects of elasticity on drying processes of polymer solutions. *Physical Review, 77*, Article 030501.
Oliver, L., & Meinders, M. B. (2011). Dynamic water vapour sorption in gluten and starch films. *Journal of Cereal Science, 54*, 409–416.
Ormondroyd, G. A., Curling, S. F., Mansour, E., & Hill, C. A. (2017). The water vapour sorption characteristics and kinetics of different wool types. *Journal of the Textile Institute, 108*, 1198–1210.
Ozawa, K., Okuzono, T., & Doi, M. (2006). Diffusion process during drying to cause the skin formation in polymer solutions. *Japanese Journal of Applied Physics, 45*, 8817.
Perdana, J., van der Sman, R. G., Fox, M. B., Boom, R. M., & Schutyser, M. A. (2014). Measuring and modelling of diffusivities in carbohydrate-rich matrices during thin film drying. *Journal of Food Engineering, 122*, 38–47.
Popescu, C. M., Hill, C. A., Curling, S., Ormondroyd, G., & Xie, Y. (2014). The water vapour sorption behaviour of acetylated birch wood: How acetylation affects the sorption isotherm and accessible hydroxyl content. *Journal of Materials Science, 49*, 2362–2371.
Popescu, C. M., Hill, C. A., & Kennedy, C. (2016). Variation in the sorption properties of historic parchment evaluated by dynamic water vapour sorption. *Journal of Cultural Heritage, 17*, 87–94.
Preston, T. C. (2022). Non-fickian diffusion in viscous aerosol particles. *Canadian Journal of Chemistry, 100*, 168–174.
Price, H. C., Mattsson, J., & Murray, B. J. (2016). Sucrose diffusion in aqueous solution. *Physical Chemistry Chemical Physics, 18*, 19207–19216.
Price, H. C., Mattsson, J., Zhang, Y., Bertram, A. K., Davies, J. F., Grayson, J. W., Martin, S. T., O'Sullivan, D., Reid, J. P., Rickards, A. M., et al. (2015). Water diffusion in atmospherically relevant $\alpha$-pinene secondary organic material. *Chemical Science, 6*, 4876–4883.
Räderer, M., Besson, A., & Sommer, K. (2002). A thin film dryer approach for the determination of water diffusion coefficients in viscous products. *Chemical Engineering Journal, 86*, 185–191.
Reese, S. (2003). A micromechanically motivated material model for the thermo-viscoelastic material behaviour of rubber-like polymers. *International Journal of Plasticity, 19*, 909–940.
Renzetti, S., Voogt, J., Oliver, L., & Meinders, M. (2012). Water migration mechanisms in amorphous powder material and related agglomeration propensity. *Journal of Food Engineering, 110*, 160–168.
Roca, E., Guillard, V., Broyart, B., Guilbert, S., & Gontard, N. (2008). Effective moisture diffusivity modelling versus food structure and hygroscopicity. *Food Chemistry, 106*, 1428–1437.
Salmén, L., & Larsson, P. A. (2018). On the origin of sorption hysteresis in cellulosic materials. *Carbohydrate Polymers, 182*, 15–20.
Siemons, I., Boom, R., Van der Sman, R., & Schutyser, M. (2019). Moisture diffusivity in concentrated and dry protein-carbohydrate films. *Food Hydrocolloids, 97*, Article 105219.
Siemons, I., Politiek, R., Boom, R., van der Sman, R., & Schutyser, M. (2020). Dextrose equivalence of maltodextrins determines particle morphology development during single sessile droplet drying. *Food Research International, 131*, Article 108988.
Siemons, I., Veser, J., Boom, R., Schutyser, M., & van der Sman, R. (2022a). *Rheological behaviour of concentrated maltodextrins describes skin formation and morphology development during droplet drying*. Food Hydrocolloids, Article 107442.
Siemons, I., Veser, J., Boom, R., Schutyser, M., & van der Sman, R. (2022b). Rheological behaviour of concentrated maltodextrins describes skin formation and morphology development during droplet drying. *Food Hydrocolloids, 126*, Article 107442.
van der Sman, R., Chakraborty, P., Hua, N., & Kollmann, N. (2023). Scaling relations in rheology of proteins present in meat analogs. *Food Hydrocolloids, 135*, Article 108195.
van der Sman, R., Jin, X., & Meinders, M. (2013). A paradigm shift in drying of food materials via free-volume concepts. *Drying Technology, 31*, 1817–1825.
van der Sman, R., & Mauer, L. J. (2019). Starch gelatinization temperature in sugar and polyol solutions explained by hydrogen bond density. *Food Hydrocolloids*. https://doi.org/10.1016/j.foodhyd.2019.03.034
Thirunathan, P., Arnz, P., Husny, J., Gianfrancesco, A., & Perdana, J. (2018). Thermogravimetric analysis for rapid assessment of moisture diffusivity in polydisperse powder and thin film matrices. *Food Chemistry, 242*, 519–526.
Townrow, S., Roussenova, M., Giardiello, M. I., Alam, A., & Ubbink, J. (2010). Specific volume- hole volume correlations in amorphous carbohydrates: Effect of temperature, molecular weight, and water content. *The Journal of Physical Chemistry B, 114*, 1568–1578.
Ubbink, J., & Dupas-Langlet, M. (2020). Rheology of carbohydrate blends close to the glass transition: Temperature and water content dependence of the viscosity in relation to fragility and strength. *Food Research International, 138*, Article 109801.
Ubbink, J., Giardiello, M. I., & Limbach, H. J. (2007). Sorption of water by bidisperse mixtures of carbohydrates in glassy and rubbery states. *Biomacromolecules, 8*, 2862–2873.
Van der Sman, R. (2012). Thermodynamics of meat proteins. *Food Hydrocolloids, 27*, 529–535.
Van der Sman, R. (2013). Modeling cooking of chicken meat in industrial tunnel ovens with the flory–rehner theory. *Meat Science, 95*, 940–957.
Van der Sman, R. (2015a). Biopolymer gel swelling analysed with scaling laws and flory–rehner theory. *Food Hydrocolloids, 48*, 94–101.
Van der Sman, R. (2015b). Hyperelastic models for hydration of cellular tissue. *Soft Matter, 11*, 7579–7591.
Van der Sman, R. (2019). Phase separation, antiplasticization and moisture sorption in ternary systems containing polysaccharides and polyols. *Food Hydrocolloids, 87*, 360–370.
Van der Sman, R., & Meinders, M. (2011). Prediction of the state diagram of starch water mixtures using the flory–huggins free volume theory. *Soft Matter, 7*, 429–442.
Van der Sman, R., & Meinders, M. (2013). Moisture diffusivity in food materials. *Food Chemistry, 138*, 1265–1274.
Van der Sman, R., Ubbink, J., Dupas-Langlet, M., Kristiawan, M., & Siemons, I. (2022). Scaling relations in rheology of concentrated starches and maltodextrins. *Food Hydrocolloids, 124*, Article 107306.
Vrentas, J., Jarzebski, C., & Duda, J. (1975). A deborah number for diffusion in polymer-solvent systems. *AIChE Journal, 21*, 894–901.
Vrentas, J., & Vrentas, C. M. (1991). Sorption in glassy polymers. *Macromolecules, 24*, 2404–2412.
Vrentas, J., & Vrentas, C. M. (1996). Hysteresis effects for sorption in glassy polymers. *Macromolecules, 29*, 4391–4396.
Wang, H., & Cai, S. (2015). Drying-induced cavitation in a constrained hydrogel. *Soft Matter, 11*, 1058–1061.
Wu, J., & Peppas, N. A. (1993). Modeling of penetrant diffusion in glassy polymers with an integral sorption deborah number. *Journal of Polymer Science Part B: Polymer Physics, 31*, 1503–1518.
Xiao, R., Sun, H., & Chen, W. (2016). An equivalence between generalized maxwell model and fractional zener model. *Mechanics of Materials, 100*, 148–153.
Yu, X., Schmidt, A. R., Bello-Perez, L. A., & Schmidt, S. J. (2008). Determination of the bulk moisture diffusion coefficient for corn starch using an automated water sorption instrument. *Journal of Agricultural and Food Chemistry, 56*, 50–58.
Zhang, X., Hu, H., & Guo, M. (2015). Relaxation of a hydrophilic polymer induced by moisture desorption through the glass transition. *Physical Chemistry Chemical Physics, 17*, 3186–3195.
Zhao, X., Li, W., Zhang, H., Li, X., & Fan, W. (2019). Reaction–diffusion approach to modeling water diffusion in glutinous rice flour particles during dynamic vapor adsorption. *Journal of Food Science & Technology, 56*, 4605–4615.
Zhu, L., Cai, T., Huang, J., Stringfellow, T. C., Wall, M., & Yu, L. (2011). Water self-diffusion in glassy and liquid maltose measured by Raman microscopy and nmr. *The Journal of Physical Chemistry B, 115*, 5849–5855.
Zobrist, B., Soonsin, V., Luo, B. P., Krieger, U. K., Marcolli, C., Peter, T., & Koop, T. (2011). Ultra-slow water diffusion in aqueous sucrose glasses. *Physical Chemistry Chemical Physics, 13*, 3514–3526.